

## THREE-DIMENSIONAL STABILITY ANALYSES OF TORNADO-LIKE VORTICES WITH SECONDARY CIRCULATIONS

David S. Nolan\*

Rosenstiel School of Marine and Atmospheric Science, University of Miami, Florida  
and

Michael T. Montgomery

Department of Atmospheric Science, Colorado State University, Fort Collins, Colorado

### 1. INTRODUCTION

A number of observed phenomena have motivated studies on the stability of intense atmospheric vortices. For tornadoes, these would include the multiple vortex and vortex breakdown phenomena. The multiple vortex phenomenon refers to the occasional appearance of smaller vortices within the larger tornadic vortex core as first hypothesized by Fujita (1971). The wind field deviations associated with asymmetries and/or smaller-scale vortices in the core of a tornado have recently been observed directly with portable Doppler radar (Bluestein and Pazmany, 2000). A vortex breakdown structure is also sometimes observed in tornadoes, with a nearly laminar, supercritical flow near the surface, and turbulent, subcritical flow aloft (Lugt, 1989).

A number of studies have identified dynamical instabilities associated with the radial shears of the azimuthal and vertical winds as the likely cause for these phenomena (e.g., Rotunno, 1978; Gall, 1983; Staley and Gall, 1984). Walko and Gall (1984) extended their stability analyses to allow for the arbitrary variation of both the basic-state flow and the perturbations with height. Unstable modes were found for an axisymmetric vortex generated in a simplified axisymmetric model, with higher azimuthal wavenumbers and more barotropic (i.e., two-dimensional) dynamics prevailing as the swirl ratio was increased.

Motivated by observations of similar phenomena in intense hurricanes, the authors have extended this type of analysis to include the effects of temperature, stratification, and density variations (Nolan and Montgomery, 2002a). Our approach is also more versatile, in that our modes are computed from the eigenvectors of a linear dynamical system, rather than by examining the linearized evolution of random initial perturbations, i.e., *all* modes, unstable or otherwise, are identified simultaneously. Furthermore, Walko and Gall (1984) used a basic-state without a swirling boundary layer, the presence of which is known to be crucial in determining the structure of the flow in the inner core of all tornado-like vortices (Rotunno, 1979; Nolan and Farrell, 1999). Thus we return to the problem of fully three-dimensional

unstable modes in tornado-like vortices.

### 2. BASIC STATE VORTEX

A tornado-like basic-state is generated from a simple numerical model of tornadogenesis: axisymmetric simulation of incompressible fluid in solid-body rotation, forced to converge by a fixed vertical forcing field at the center of the domain. Such vortices have been studied extensively and are known to reproduce many of the observed features and behaviors of actual tornadoes (Fiedler, 1993; Nolan and Farrell, 1999). The model parameters have been chosen to produce a "drowned vortex jump," as shown in Fig. 1. The variables are nondimensional, with a background rotation rate  $\Omega=0.2$ , a constant eddy viscosity  $\nu=0.0005$ , and a convective velocity scale  $U=1.0$ . The fields are averaged over a suitable period of time so as to smooth out any transient features.

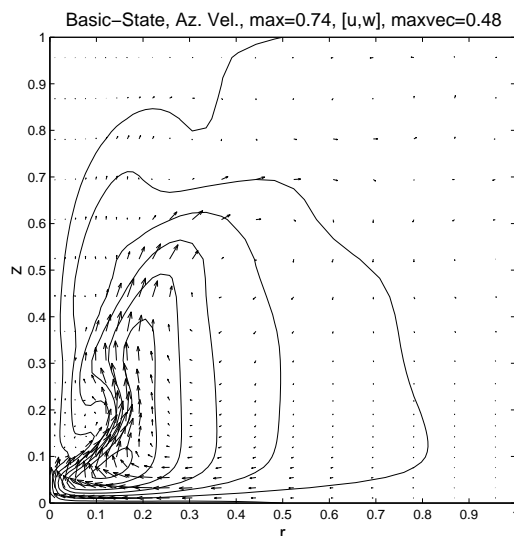


Figure 1: Basic-state tornado-like vortex, with secondary circulation. Structure of the stretched grid is also shown.

### 3. THE ASYMMETRIC TORNADO-HURRICANE EQUATIONS

Due to space limitations, we cannot provide a complete analysis of the equations, but we will instead describe the general approach; details are available in Nolan and Montgomery (2002a). We start with the anelastic momentum equations for dry adiabatic motions in cylindrical coordinates. These are comprised of the

\* Corresponding author address: Prof. David S. Nolan, RSMAS/MPO, University of Miami, 4600 Rickenbacker Causeway, Miami, FL 33149. email: dnolan@rsmas.miami.edu

momentum equations for the radial ( $u$ ), azimuthal ( $v$ ), and vertical winds ( $w$ ), the conservation of potential temperature ( $\theta$ ), and the anelastic (density weighted) incompressibility condition. For the purposes of generality, the effects of temperature and density variations and the earth's rotation are included in the present exposition. The equations are linearized for small perturbations about the basic-state flow, and these perturbations are assumed to have the form

$$v'(r, \lambda, z, t) = v_n(r, z, t)e^{in\lambda}, \quad (1)$$

such that all variables vary exponentially in the azimuthal direction for some wavenumber  $n$ , but may have arbitrary structure in time and in the radial and vertical directions. After linearization and substitution for the perturbation variables in the form of (1), we have:

$$\frac{\bar{D}u_n}{Dt} + u_n \frac{\partial \bar{u}}{\partial r} + w_n \frac{\partial \bar{u}}{\partial z} - (2\bar{\Omega} + f)v_n = -\frac{1}{\bar{\rho}} \frac{\partial p_n}{\partial r}, \quad (2)$$

$$\frac{\bar{D}v_n}{Dt} + w_n \frac{\partial \bar{v}}{\partial z} + \left( \frac{\partial \bar{v}}{\partial r} + \bar{\Omega} + f \right) u_n + \frac{\bar{u}}{r} v_n = -\frac{1}{\bar{\rho}} \frac{in}{r} p_n, \quad (3)$$

$$\frac{\bar{D}w_n}{Dt} + u_n \frac{\partial \bar{w}}{\partial r} + w_n \frac{\partial \bar{w}}{\partial z} = -\frac{1}{\bar{\rho}} \frac{\partial p_n}{\partial z} + g \frac{\theta_n}{\bar{\theta}}, \quad (4)$$

$$\frac{\bar{D}\theta_n}{Dt} + u_n \frac{\partial \bar{\theta}}{\partial r} + w_n \frac{\partial \bar{\theta}}{\partial z} = 0, \quad (5)$$

$$\frac{1}{r\bar{\rho}} \frac{\partial}{\partial r} (r\bar{\rho}u_n) + \frac{in}{r} v_n + \frac{1}{\bar{\rho}} \frac{\partial}{\partial z} (\bar{\rho}w_n) = 0, \quad (6)$$

where  $g$  is the gravitational acceleration,  $f$  is the Coriolis parameter,  $\bar{\rho}$  is the (fixed) anelastic density field,  $p_n$  is the perturbation pressure,  $\bar{\Omega} = \bar{v}/r$  is the basic-state angular velocity, and the basic-state material derivative is

$$\frac{\bar{D}}{Dt} = \frac{\partial}{\partial t} + \bar{u} \frac{\partial}{\partial r} + in\bar{\Omega} + \bar{w} \frac{\partial}{\partial z}. \quad (7)$$

We refer to (2)-(7) as the *asymmetric tornado-hurricane equations*. Since hurricanes can be represented to first order as a vortex in gradient wind and hydrostatic balance, with no secondary circulation, we call these equations with  $\bar{u}(r, z) = \bar{w}(r, z) = 0$  the *asymmetric hurricane equations*. Alternatively, since the dynamics of tornadoes are represented accurately by an incompressible vortex driven by overhead convection, we shall call the equations with  $\bar{\rho}(r, z)$  constant, and (5) neglected, the *asymmetric tornado equations*. Diffusion terms have been omitted for brevity, but are included in the equations.

Observe that there are no derivatives operating on  $v_n$  in (6), such that  $v_n$  can be eliminated in favor of  $u_n$  and  $w_n$ . The same applies for  $p_n$  in (3), and thus  $p_n$  may also be eliminated. Through various manipulations we are left with three coupled, linear equations for  $u_n$ ,  $w_n$ , and  $\theta_n$ . Note that this approach cannot be used for  $n=0$ ; in this case,  $p_n$  may be eliminated through the use of a streamfunction  $\psi_n$ , leading to three equations for  $\psi_n$ ,  $v_n$ , and  $\theta_n$ .

Symmetric dynamics and instability will be discussed in future work (Nolan and Montgomery, 2002b).

#### 4. NUMERICAL SOLUTION

Through standard techniques, the asymmetric tornado equations are discretized into the linear dynamical system

$$\frac{dx}{dt} = \mathbf{A}x, \quad (8)$$

where  $x$  is a column vector whose elements contain the values of each of  $u_n$  and  $w_n$  at each gridpoint. The modes of the system are the eigenvectors of  $\mathbf{A}$ .

Some practical difficulty lies in the size of the matrix  $\mathbf{A}$ . The domain needs to be large enough so that the outer boundary does not overly influence the inner-core modes. Using a regularly spaced grid, one might need as much as 100 points in each of the radial and vertical directions for sufficient resolution of the inner-core flow shown in Fig. 1. The size of  $\mathbf{A}$  would then be on the order of 20000x20000. To overcome this difficulty we use grids that are stretched in both the radial and vertical directions, such that a large number of gridpoints are packed into the lower levels of the inner core of the vortex. For the calculations presented here, the grid has an Arakawa C structure with 40x40 points, with minimum grid spacings of 0.011 in the corner flow region, stretching to 4 times larger in the far-field. The shape of the grid, but with only 20x20 points, is also shown in Fig. 1 by the locations of the flow vectors.

#### 5. UNSTABLE MODES IN TORNADO-LIKE VORTICES

For our analysis of the vortex in Fig. 1, we use the asymmetric tornado equations with no-slip boundary conditions at the lower surface,  $f=0$ , and a constant  $\rho=1$ . The viscosity is the same as that used in the axisymmetric model that generated the basic-state. Also incorporated into the dynamics are damping regions near the upper and outer boundaries, aka "sponges," which suppress instabilities in the inertially unstable outflow layer, so that we may focus on the inner-core dynamics of the vortex.

The growth rates of the most unstable modes in the core of the tornado-like vortex are shown in Fig. 2 (circles). Robustly unstable modes are found for  $n=1$  and  $n=2$ , with  $e$ -folding times of 6.75 and 3.58, respectively, (compared to a vortex circulation time of 2.2). The structure of the  $n=2$  unstable mode is shown in Fig. 3, in terms of the magnitude of the perturbation azimuthal velocity in the  $r$ - $z$  plane, and horizontal cross-sections of the vertical vorticity and velocity at  $z=0.29$ . The mode is normalized to have maximum  $u_n=1.0$ . The mode has a vorticity structure somewhat similar to modes associated with changes in sign of the basic-state vertical vorticity gradient, discussed by Michaelke and Timme (1967) and Schubert et al. (1999), but it also has large vertical velocity perturbations and its vertical structure changes significantly with height (not shown).

In previous work, considerable attention has been

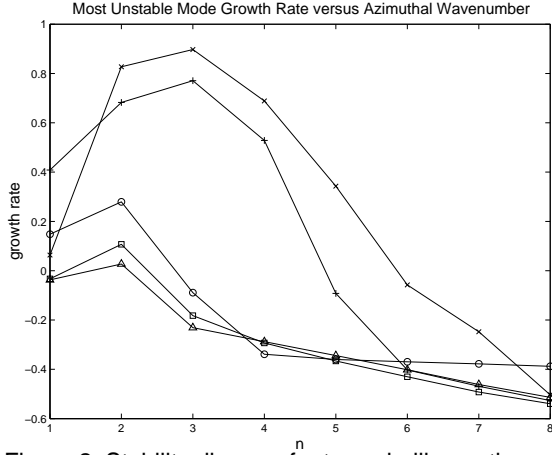


Figure 2: Stability diagram for tornado-like vortices:  
o: tornado-like vortex shown in Fig. 1;  
+: vertically periodic vortex with  $v$  and  $w$  profiles from  $z = 0.225$ ; x: periodic vortex with  $v$  and  $w$  profiles from  $z = 0.375$ ;  
tri: periodic vortex with  $v$  profile (only) from  $z = 0.225$ ; sq: periodic vortex with  $v$  profile from  $z = 0.375$ .

given towards determining whether these modes owe their existence to the radial or vertical shears of the azimuthal or vertical winds. A budget equation for the production of perturbation kinetic energy may be used for this purpose, where

$$\begin{aligned} \frac{\partial E'}{\partial t} = & -\iiint \left\{ \left[ u'v' \left( \frac{\partial \bar{v}}{\partial r} - \frac{\bar{v}}{r} \right) \right]_{vr} + \left[ u'w' \frac{\partial \bar{w}}{\partial r} \right]_{wr} \right. \\ & + \left[ u'u' \frac{\partial \bar{u}}{\partial r} + v'v' \frac{\bar{u}}{r} \right]_{ur} + \left[ v'w' \frac{\partial \bar{v}}{\partial z} \right]_{vz} \\ & + \left[ w'w' \frac{\partial \bar{w}}{\partial z} \right]_{wz} + \left[ u'w' \frac{\partial \bar{u}}{\partial z} \right]_{uz} \\ & \left. + [u'F_r' + v'F_\lambda' + w'F_z']_F \right\} 2\pi r dr d\lambda dz \end{aligned} \quad (9)$$

[see, e.g., Walko and Gall (1984), except for a correction to their term 3]. The terms are labelled according to the wind field and direction of momentum transport they represent. The three dominant sources of KE for the most unstable mode are shown in Fig. 4, which are the  $wr$ ,  $wz$ , and  $vz$  terms, with 0.016, 0.0087, and 0.0038 units of KE production, respectively. Remarkably, the  $vr$  term, associated with barotropic instability, comes in fourth place with 0.0025 units, though its largest local values are twice those of the  $vz$  term (not shown). The  $ur$  and  $uz$  terms contribute 0.0021 and -0.00011 units, respectively.

The stability of the 3D, axisymmetric vortex may also be compared to similar vortices which do not vary with height. For this purpose, vertically periodic vortices were constructed with the same  $v(r)$  and  $w(r)$  profiles as the tornado-like vortex at heights where the unstable mode is particularly active,  $z = 0.225$  and  $z = 0.375$ . The same numerical model is used, but with vertically periodic boundary conditions. While this forces the vertical

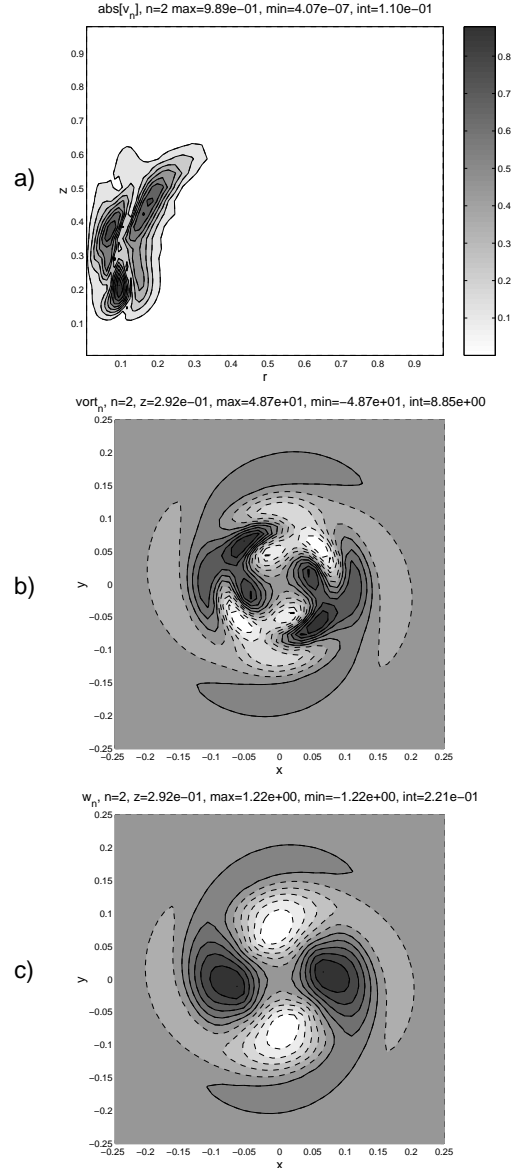


Figure 3: The most unstable mode for the tornado-like vortex: a) complex magnitude of  $v_n$ ; b) horizontal slice of the vertical vorticity; c) horizontal slice of the vertical velocity.

wavelengths of the modes to be either 1, 1/2, 1/3, etc., calculations with varying vertical domain sizes gave similar results. Stability curves for the two vertically periodic vortices are shown in Fig. 2. The periodic vortices are more unstable and have most unstable modes for  $n = 3$  and are also unstable for higher wavenumbers. All the most unstable modes have vertical wavenumbers of either 1 or 2 (relative to the vertical domain size, 1.0), with the higher vertical wavenumber preferred for the higher azimuthal wavenumbers. Also shown are calculations for vortices using  $v(r)$  only. These vortices are much less unstable, consistent with the findings of the energy production calculations.

We are left with the question as to why the tornado-

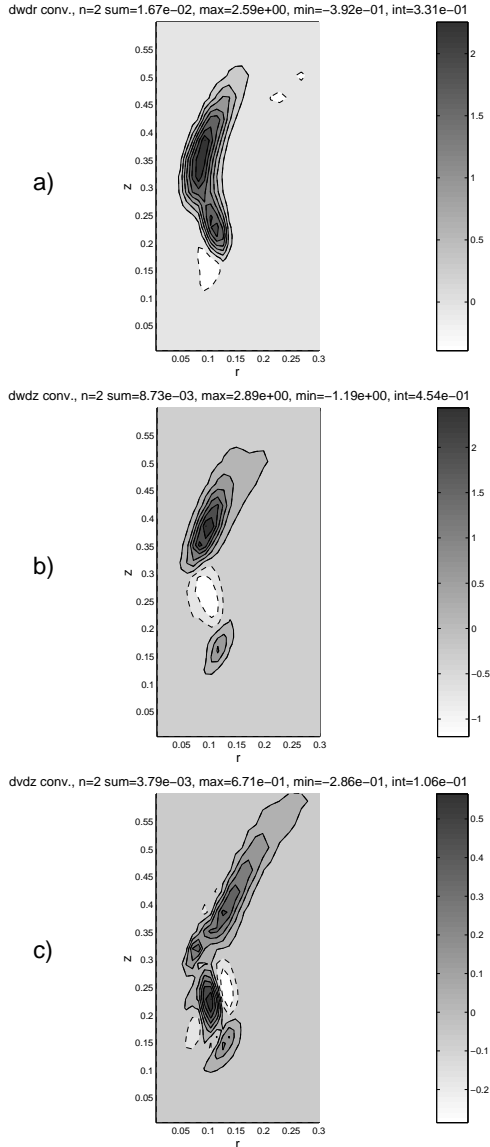


Figure 4: Kinetic eddy production for the most unstable mode: a)  $wr$  term; b)  $wz$  term; c)  $vz$  term; see text for explanation.

like vortex is considerably less unstable than its vertically periodic counterparts. The answer is undoubtedly strongly related to the fact that the most unstable vertical wavelengths are comparable to the distance over which the vortex maintains significant radial shears of the azimuthal and vertical winds. Below this region, there is the swirling boundary layer, and above, the vortex expands and weakens. Vertical propagation also plays a role: higher wavenumber modes generally have lower phase and group speeds, and thus are not able to propagate downwards fast enough to stay in the unstable region.

## 6. DISCUSSION

We have extended atmospheric vortex stability analysis to the problem of three-dimensional, asymmetric dynamics of tornado-like vortices and their strong sec-

ondary circulations. We find that robust instabilities are present in these vortices, whose existence appear to rely most strongly on the radial shear of the vertical wind. Comparisons to vertically periodic vortices, and previous results for vortices without boundary layers (Walko and Gall, 1984), indicate that strong vertical advection may prohibit higher-wavenumber instabilities. This demonstrates the importance of resolving the boundary layer, which contributes greatly to the mass flux of the axial flow. Instabilities in higher-swirl vortices will be studied in the future.

## 7. ACKNOWLEDGEMENTS:

This work was supported by the Office of Naval Research under contract N00014-93-1-0456 P0006, Colorado State University, Princeton University, NOAA, and the NSF under grant ATM-0132006.

## REFERENCES:

- Bluestein, H. B., and A. Pazmany, 2000: Observations of tornadoes and other convective phenomena with a mobile, 3-mm wavelength Doppler radar. *Bull. Amer. Met. Soc.*, **81**, 2939-2951.
- Fujita, T. T., 1971: Proposed mechanism of suction spot accompanied by tornadoes. *7th Conf. on Severe Local Storms. Kansas City, MO. AMS.*
- Fiedler, B. H., 1993: Numerical simulation of axisymmetric tornadogenesis in forced convection. In *The Tornado: its structure, dynamics, prediction, and hazards*. C. Church, et al., eds., AGU.
- Gall, R. L., 1983: A linear analysis of the multiple vortex phenomenon in simulated tornadoes. *J. Atmos. Sci.*, **40**, 2010-2024.
- Lugt, H. J., 1989: Vortex breakdown in atmospheric columnar vortices. *Bull. Amer. Met. Soc.*, **12**, 1526-1527.
- Michaelke, A., and A. Timme, 1967: On the inviscid instability of certain two-dimensional vortex-type flows. *J. Fluid Mech.*, **29**, 647-666.
- Nolan, D. S., and B. F. Farrell, 1999: The structure and dynamics of tornado-like vortices. *J. Atmos. Sci.*, **56**, 2908-2936.
- Nolan, D. S., and M. T. Montgomery, 2002a: Three-dimensional, nonhydrostatic perturbations to balanced, hurricane-like vortices. Part I: Linearized formulation, stability, and evolution. To appear in *J. Atmos. Sci.*
- Nolan, D. S., and M. T. Montgomery, 2002b: Three-dimensional, nonhydrostatic perturbations to balanced, hurricane-like vortices. Part II: Symmetric dynamics and nonlinear simulations. Submitted to *J. Atmos. Sci.*
- Rotunno, R., 1978: A note on the stability of a cylindrical vortex sheet. *J. Fluid Mech.*, **87**, 761-771.
- Rotunno, R., 1979: A study in tornado-like vortex dynamics. *J. Atmos. Sci.*, **36**, 140-155.
- Schubert, W. H., M. T. Montgomery, R. K. Taft, T. G. Guinn, S. R. Fulton, J. P. Kossin, and J. P. Edwards, 1999: Polygonal eyewalls, asymmetric eye contraction, and potential vorticity mixing in hurricanes. *J. Atmos. Sci.*, **56**, 1197-1223.
- Staley, D. O., and R. L. Gall, 1984: Hydrodynamic instability of small eddies in a tornado vortex. *J. Atmos. Sci.*, **41**, 422-429.
- Walko, R., and Gall, R., 1984: A two-dimensional linear stability analysis of the multiple vortex phenomena. *J. Atmos. Sci.*, **41**, 3456-3471.